

Acousto-optic tunable second harmonic generation in aperiodically poled LiNbO_3

HUAXIN ZHU, YAN KONG*, TONGTONG WANG^a, JINSONG GAO^a

School of Science, Jiangnan University, Wuxi, Jiangsu 214122, China

^a*Key Laboratory of Optical System Advanced Manufacturing Technology, Changchun Institute of Optics, Fine Mechanics and Physics, Chinese Academy of Sciences, Changchun 130033, China*

We proposed a method to simultaneously implement quasi-phase-matching (QPM) second harmonic generation (SHG) and acousto-optic (AO) polarization rotation for arbitrary wavelengths in an aperiodically poled lithium niobate (APPLN). Self-adjusting algorithm (SA) is employed for designing the aperiodic microstructure. The QPM SHG and AO polarization rotation are coupled together. The numerical simulation shows that there is a competition between the SHG and AO polarization rotation, which is dominated by the acoustic intensity, that makes the output tunable.

(Received April 17, 2014; accepted March 19, 2015)

Keywords: Nonlinear optics, Electro-optic coupling, Frequency doubling, Quasi-phase matching

1. Introduction

With the development of room-temperature poling technology, it is possible to achieve domain-inverting structure in ferroelectric crystals such as LiNbO_3 , LiTaO_3 and KTiOPO_4 . In these crystals, nonlinear coefficient, piezoelectric coefficient and electro-optical coefficient will change their sign owing to the domain-inverting structure [1-4]. When two or more parameters are modulated together, that could result in some coupling effects. In recent years, the cascading of two different interactions within a single optical superlattice has been attracting more and more interest and research attention, which has been demonstrated to have an advantage over a single one [5-8]. Cascaded frequency doubling and acousto-optic (AO) coupling in a single periodically poled lithium niobate (PPLN) have been proposed [8]. In comparison with the electric field for electric-optical SHG tuning, the cross-field excited AO driving voltage is greatly reduced.

There are two effective ways to induce the acoustic wave. One is importing from an external transducer and the other is self-generation with a direct radio frequency (RF) signals in a PPLN acoustic superlattice. The external source solution is very flexible but the latter one is more compact, simple and efficient. However, the disadvantage is that it only happens when the quasi-phase-matching curves of the two processed coincide each other. The condition is only satisfied for a set of fundamental wavelengths and a period of PPLN under certain temperature circumstance. It is still a question that SHG and AO polarization coupling can occur simultaneously for arbitrary wavelength at a given temperature.

In order to solve the above problem, we propose the use of aperiodically poled lithium niobate (APPLN) to realize the cascading of arbitrary SHG and AO polarization coupling. Self-adjusting (SA) algorithm is proposed to design the required aperiodic structure, where the wave vector mismatch of each individual process is compensated for by multiple reciprocal vector provided by the APPLN.

2. The coupling equations

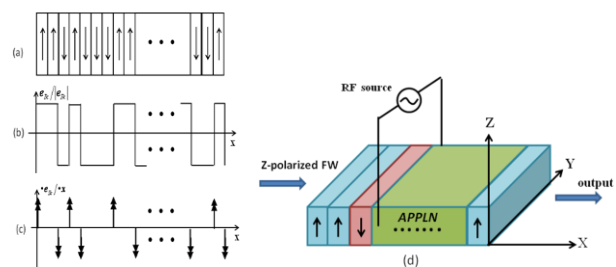


Fig. 1. Schematic diagram of APPLN: (a) polarization directions of positive or negative domains (b) piezoelectric tensor elements; (c) spatial derivative of piezoelectric tensors elements understood as acoustic sources; (d) Integrated APPLN/AO tunable frequency double with cross-field RF driving.

Superlattices in LiNbO_3 has the spontaneous polarization parallel [Fig. 1(a)] to the domain walls. The crystal unit cells of domains with anti-parallel spontaneous

polarization are congruent and can be transformed into each other by a 180° rotation about the x axis. Thus, on inversion, the z changes sign, which results in change of sign for all odd-ranked tensor elements, e.g., nonlinear coefficients or piezoelectric coefficients e_{jk} [Fig. 1(b)]. Here we consider an x-propagating longitudinal acoustic wave excited by a cross-field RF signal. The domain boundaries of the acoustic superlattice can be viewed as alternating δ -function source of the acoustic field [Fig. 1(c)]. A schematic diagram of AO polarization rotation and SHG in the APPLN with cross-field RF driving is shown in Fig. 1(d). In this paper, “ \uparrow ” represent the positive domain, “ \downarrow ” represent the negative domain. The poling direction is along the z-axis of the crystal. A cross-field RF driving signal is applied at the Y-side surface to excite longitudinal wave along X-axis. When different collinear acoustic waves travel in it along X-axis, the refractive index modulation is built up due to the elasto-optic effect, which could induce the acousto-optic (AO) polarization rotation. Here we assume the second harmonic (SH) wave's polarization is rotated. The input light is a Z-polarized fundamental wave (FW). The coupling equations ($\omega_{1z} \rightarrow \omega_{2z}$, $\omega_{2z} \rightarrow \omega_{2y}$) including both the frequency doubling and the AO coupling can be deduced as follows [8]:

$$\begin{cases} \frac{dE_{1z}}{dx} = -i \frac{\omega_1 d_{33}(x)}{n_{1z} c} E_{2z} E_{1z}^* e^{i\Delta k_1 x} \\ \frac{dE_{2z}}{dx} = -i \frac{\omega_2}{2n_{2z} c} d_{33}(x) E_{1z}^2 e^{-i\Delta k_1 x} - i \frac{\omega_2}{4n_{2z} c} n_{2y}^2 n_{2z}^2 p_{41} S(x) E_{2y} e^{i\Delta k_2 x} \\ \frac{dE_{2y}}{dx} = -i \frac{\omega_2}{4n_{2y} c} n_{2y}^2 n_{2z}^2 p_{41}(x) E_{2z} e^{-i\Delta k_2 x} \end{cases} \quad (1)$$

With $d_{33}(x) = d_{33} f(x)$, $S(x) = S \cdot f(x) = e_{22} E_{\pm y} f(x)$, $\Delta k_1 = k_{2z} - 2k_{1z}$, $\Delta k_2 = k_{2y} - k_{2z}$.

Here $E_{j\xi}$, $\omega_{j\xi}$, $k_{j\xi}$ and $n_{j\xi}$ (the subscripts $j=1,2$ refer to FW and SH, respectively, and $\xi = y, z$ represent the polarization) are the electric field, the angular frequencies, the wave-vectors and the refractive indices, respectively. c is the speed of light in vacuum; d_{33} is the nonlinear coefficient; p_{41} is the corresponding elasto-optic coefficient. S is the amplitude of strain. Note that $E_{\pm y}$ is a scalar, $S(x) = e_{jk} E_{\pm y}$ is still a three-ranked tensor. $f(x)$ is the structure function of APPLN, and it can be expanded through Fourier transformation[7]:

$$f(x) = \sum_m g_m \exp(-iG_m x) \quad (2)$$

where G_m are the reciprocal vectors and g_m are the amplitude of reciprocal vectors. If G_1 and G_2 are provided by an APPLN, with $G_1 = \Delta k_1$, $G_2 = \Delta k_2$, where they phase-match the SHG and AO polarization rotation process, the coupling equations can be deduced to be

$$\begin{cases} \frac{dA_{1z}}{dx} = -iK_1 A_{1z}^* A_{2z} \\ \frac{dA_{2z}}{dx} = -\frac{i}{2} K_1 A_{1z}^2 - iK_2 A_{2y} \\ \frac{dA_{2y}}{dx} = -iK_2^* A_{2z} \end{cases} \quad (3)$$

$$\text{With } A_j = \sqrt{\frac{n_j}{\omega_j}} E_j, K_1 = \frac{d_{33} g_1}{c} \sqrt{\frac{\omega_2^2 \omega_1}{n_{1z}^2 n_{2z}}}, K_2 = \frac{\omega_1 (n_{1y} n_{1z})^{3/2} p_{41} g_2 S}{4c}.$$

3. Self-adjusting algorithm

Here we would utilize the self-adjusting algorithm to search a specific structure, in which the reciprocals could be equal to the phase mismatching of the two processes. The prototype of the SA algorithm was first proposed and discussed in the previous literature by Ming Lu et al [9]. The crystal is divided into N unit blocks, deriving from the Fourier transformation the magnitude of each reciprocal which can be written as

$$|g_m| = \left| \frac{1}{L} \int_0^L f(x) e^{iG_m x} dx \right| = \frac{1}{L \Delta k'(x)} \left| \sum_{q=0}^{N-1} d(z_q) \left(e^{i\Delta k'(x) z_{q+1}} - e^{i\Delta k'(x) z_q} \right) \right| \quad (4)$$

Then we define a new set of vectors $U_q(m)$, where $U_q(m) = e^{i\Delta k'(m) z_{q+1}} - e^{i\Delta k'(m) z_q}$, and $m=1, 2, \dots$ represent $\lambda_1, \lambda_2, \dots$. It can be easily proved that $U_q(m)$ are of the same module for certain wavelength. Thus we rearrange Eq. (4) as

$$|g_m| = \frac{1}{L \Delta k'(m)} \left| \sum_{q=0}^{N-1} d(z_q) U_q \right| \quad (5)$$

In order to obtain the largest magnitude of the specific reciprocal, $d(z_q)$ is to be optimized that the right-hand side of Eq. (5) approaches its maximum. In the algorithm, we assume the polarization orientation of the first unit block to be positive. For the second block, if $|\sum_m U_0(m) + \sum_m U_1(m)| > |\sum_m U_0(m) - \sum_m U_1(m)|$, the second block should be positive; otherwise negative; as shown in Fig. 2. Generally, with the N th block, comparison of $|\sum_m \sum_{n=0}^{N-2} U_n(m) + \sum_m U_{N-1}(m)|$ with $|\sum_m \sum_{n=0}^{N-2} U_n(m) - \sum_m U_{N-1}(m)|$ will determine its polarization orientation. Repeating the procedure along the crystal yields the final APPLN structure.

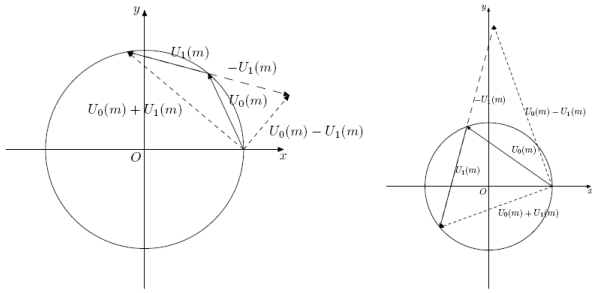


Fig. 2. The selection criteria of the poled direction. $U_1(m)$ corresponds to positive poled direction, and negative poled direction, of the second unit domain block.

To be specific, we consider building an APPLN with certain reciprocals pre-determined by the SHG and AO processes. We assume the fundamental wavelength to be 1550 nm, the crystal 2 cm long and divided into 4000 congruent unit blocks. Certainly you can choose the fundamental wavelength, the length of crystal and each block arbitrarily as long as you want. Moreover, the refractive indices of the fundamental and second harmonic depend on the Sellmeier equations [10-11] and the temperature is assigned to be 25°C. For the case discussed in this paper, the calculation result is shown in Fig. 3. As can be seen, the values of g_1 and g_2 are 0.4639 and 0.1710, respectively. It should be mentioned that the method could be suit for arbitrary two or more SHG and polarization coupling processes. For any wavelength in the transparency range of the crystal and for a given temperature, a proper structure can always be obtained using SA algorithm to simultaneously implement SHG and AO polarization rotation.

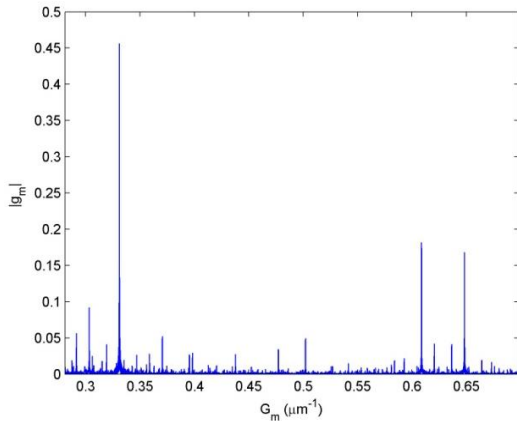


Fig. 3. The amplitude of the reciprocal vectors provided by the APPLN.

4. Numerical simulations

When the SHG and AO polarization rotation are phase-matched within the same crystal, the two processes would compete with each other, which leads to a

continuous energy transfer among the FW and SHs. The coupling depends on both the acoustic intensity and the input FW intensity, which can be seen as a tunable control, as Eq. (3) shows. In this section, we will investigate the normalized intensity of three waves with APPLN under different acoustic intensity and input FW intensity conditions.

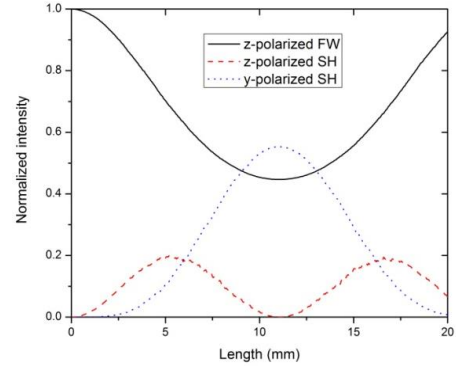


Fig. 4. Normalized light intensities versus the APPLN length under the phase-matching conditions. Here the pump FW intensity and acoustic wave intensity are 10 MW/cm² and 0.11 MW/cm², respectively.

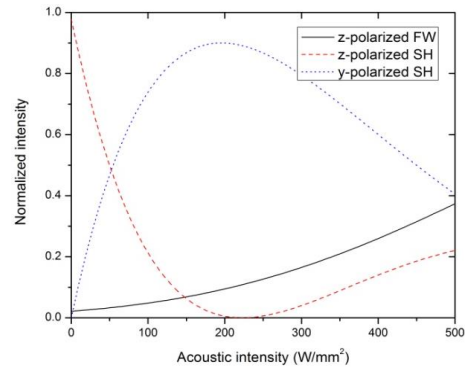


Fig. 5. Normalized light intensities as a function of the acoustic intensity. Here the pump FW intensity is set to be 10 MW/cm².

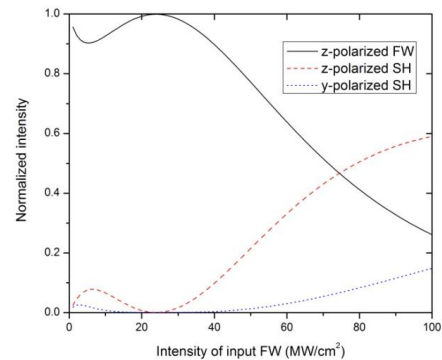


Fig. 6. Normalized light intensities versus input fundamental intensity. Here the acoustic wave intensity is 0.11 MW/cm².

Using the structure that searched by the self-adjusting algorithm, we solve the coupling equations. The simulation conditions are the same as those in the section discussing the self-adjusting algorithm. Fig. 4 shows the calculated three-wave conversion efficiency along the APPLN. Fig. 5 shows the calculated three-wave conversion efficiency as a function of the acoustic intensity. Z-polarized SH can be adjusted in the range between 0~1, Y-polarized SH can be adjusted in range between 0~0.9. Only the normalized intensity of Y-polarized SH is 0.1 lower than the results of reference [8]. The remaining results can achieve the same effects of reference [8]. The corresponding acoustic intensity is $I_a = \rho v^3 |S|^2 / 2$, where $\rho = 4640 \text{ kg/m}^3$, $v = 6570 \text{ m/s}$ are used for calculation. The final output efficiency of three waves versus input FW intensity with the same acoustic intensity is plotted in Fig. 6. When the input FW intensity is less than 40 MW/cm^2 , the output is not sensitive to the input intensity. With the increasing of the input FW intensity, the output will change greatly.

As shown above, a different acoustic intensity corresponds to different coupling coefficient κ_2 , and so to the ratio of SHG and AO polarization coupling coefficients, and finally leads to different coupling behavior. Besides the acoustic intensity, high intensity of input FW will also affect the coupling process. That is, by adjusting the acoustic intensity and the input FW intensity, the coupling process changes, and then a required SH intensity could be obtained. The light's phases and polarization are manipulated consequently.

5. Conclusion

In summary, we studied the photon-phonon interactions in a typical QPM material, the aperiodically poled LiNbO₃(APPLN). The APPLN can satisfy simultaneously the QPM conditions of the SHG and AO for arbitrary wave at a given temperature. A method called the self-adjusting algorithm is proposed to design the aperiodic microstructure, where the wave vector mismatch of each individual process is compensated by multiple reciprocal vectors provided by the APPLN. A three-wave-coupling approach is proposed to study the optical power transferring among the FW and SHs. Numerical simulation shows that the coefficient ratio can be adjusted by the tunable radio frequency(RF) signal and the input FW

intensity, so frequency doubling and polarization control can be achieved simultaneously.

Acknowledgements

This research was financially supported by the Natural Science Foundations of Jiangsu Province (No.BK20130162 and No. BK20130116) and the National Natural Science Foundation of China(No. 21206053) and the fundamental Research Funds for the Central Universities (JUSRP211A19).

References

- [1] M. Yamada, N. Nada, M. Saitoh, K. Watanabe, Appl. Phys. Lett. **62**, 435 (1993).
- [2] Y. Q. Lu, Y. Y. Zhu, Y. F. Chen, S. N. Zhu, N. B. Ming, Y. J. Feng, Science **284**, 1822 (1999).
- [3] Xianfeng Chen, Jianhong Shi, Yuping Chen, Yiming Zhu, Yuxing Xia, Yingli Chen, Opt. Lett **21**, 2115 (2003).
- [4] H. Gnewuch, N. K. Zayer, C. N. Pannell, G. W. Ross, P. G. R. Smith, Opt. Lett. **25**, 305 (2000).
- [5] C. P. Huang, Q. J. Wang, Y. Y. Zhu, Appl. Phys. B **80**, 741 (2005).
- [6] Y. Kong, X. F. Chen, Y. Xia, Appl. Phys. B **91**, 479 (2008).
- [7] Y. Zheng, Y. Kong, X. Chen, Appl. Phys. B **95**, 697 (2009).
- [8] Zi-yan Yu, Fei Xu, Fei Leng, Xiao-shi Qian, Xiang-fei Chen, Yan-qing Lu, Opt. Express **17**, 11965 (2009).
- [9] Ming Lu, Xianfeng Chen, Yuping Chen, Yuxing Xia, Appl. Opt. **46**, 4138 (2007).
- [10] G. J. Edwards, M. Lawrence, Opt. Quantum Electro. **16**, 373 (1984).
- [11] Dieter H. Jundt, Opt. Lett. **22**(20), 1553 (1997).

*Corresponding author: ykong80@163.com